DETECTING AND DATING POSSIBLY DISTINCT STRUCTURAL BREAKS IN THE COVARIANCE STRUCTURE OF FINANCIAL ASSETS

Farah Daniela Mugrabi

LIDAM Discussion Paper LFIN
2023 / 01

UCLouvain

LIDAM
LFIN | Louvain Institute of Data Analysis and Modeling in economics and statistics

LFIN

Voie du Roman Pays 34, L1.03.01 B-1348 Louvain-la-Neuve

Tel (32 10) 47 43 04

Email: lidam-library@uclouvain.be

https://uclouvain.be/en/research-institutes/lidam/lfin/publications.html

Detecting and dating possibly distinct structural breaks in the covariance structure of financial assets

Farah Daniela Mugrabi[a]

[a] *Université Catholique de Louvain, Louvain Finance Institute.*

Abstract

This paper aims to identify and date contagion by accounting for possibly distinct structural breaks among the covariance structure of financial assets. We propose an efficient three-steps procedure that applies the Lagrange Multiplier test, in particular the *SupLM* statistic, among the DCC-GARCH model parameters. Monte Carlo experiments show that our procedure possess good power and accurately detects the location of the true breaking points. We explore contagion between the government bond and stock markets of advanced and emerging economies. Evidence of common shifts in the covariance structure coincides with the European Sovereign Debt Crisis, the Taper Tantrum originated in United States in mid-2013 and the Covid-19 pandemic.

Keywords: contagion, emerging markets, unknown structural breaks, Lagrange Multiplier test, DCC-GARCH model.

JEL Classification: C32, C15, G15.

Email address: `farah.mugrabi@uclouvain.be` (Farah Daniela Mugrabi)

Acknowledgements: This research has been funded by the Université Catholique Louvain, Grant ARES-CCD. I would like to thank Prof. Bertrand Candelon for his support, trust and encouragement. I am grateful for valuable comments and suggestions on earlier drafts from Prof. Christian M. Hafner, Prof. Sami Ben Naceur, Prof. Frédéric Vrins and colleagues from Louvain Finance Institute. The responsibility for any errors and shortcomings in this paper remains mine.

1. Introduction

There is a reasonably large amount of empirical research that has been done with regards to the existence of contagion during financial crises. The most widely used definition is $shift-contagion$ introduced in Forbes & Rigobon (2002). However, almost twenty years later, Rigobon (2019) noted that the definition of contagion is still tenuous. The author remarks that $shift - contagion$ is defined as a significant increase in the correlation between two assets attributed to a structural break originated after a crisis. Furthermore, he argues that correlation is not an unbiased estimator under the presence of heteroscedasticity or a break in the volatility structure.

Detecting structural breaks affecting specific subsets of parameters permits to differentiate $shift - contagion$ from a volatility shift. In this sense, under the assumption that the dates are unknown, the partial sample estimation (PSE), introduced in Andrews (1993), allows the detection of a single break affecting a subset of parameters. Later on, Bai & Perron (1998) and Perron et al. (2006) extend the analysis to the case of multiple structural changes and present an efficient algorithm, i.e. the *repartition* procedure. However, as noticed in Oka & Perron (2018), all of these procedures are based on the assumption that a group of parameters is affected by common breaks while the rest remains unchanged among all the sample period.

Blatt et al. (2015) finds that, during the European Sovereign Debt crisis, the variance structure increases due to increased market volatility, while $shift - contagion$ takes place later on. Thus, all the subsets may be affected by possibly distinct break dates. To this end, the authors follow the *distinctiveness* procedure proposed in Oka & Perron (2018). By employing the LR test statistic, they estimate the breakpoints affecting each individual parameter separately. As follows, they simulate a sufficiently large amount of sample partitions to determine whether the detected breaks are common or distinct. As can be seen, these methods entail computationally intensive simulations to assess critical values (see Estrada et al., 2015).

We propose an efficient procedure for multiple and possibly distinct break detection that tailors the $SupLM$ test statistic, introduced in Andrews (1993). Our three-step segmentation algorithm ($TSSA$) consists on, first, employing a bootstrapped *repartition* procedure to detect sequential breaks affecting each individual parameter. As follows, if the null hypothesis of non-breaking points is rejected for more than one parameter, we intent to determine whether the detected changes are significantly distinct as in Oka & Perron (2018). In the last step, the detection of structural breaks affecting the correlation structure is subject to the breaking points found in the variance terms.

The main advantage of the $SupLM$ statistic relies on its parsimony and asymptotic power. For the former, the statistic requires only to compute the score functions of the restricted model. Also, unlike the $SupLR$ or $SupWald$ that require parameter estimation for every partitioned sample, it makes use of the full-sample estimators. Furthermore, Andrews & Ploberger (1994) proves that $ExpLM$ has the greatest asymptotic power, property that is transferred to the $SupLM$ which is an extreme form of the optimal exponential test.

We perform Monte Carlo simulations to evaluate the performance of $TSSA$ when it is devoted to detect structural breaks among DCC-GARCH model parameters. One of the advantages of the DCC-GARCH framework, widely used in the financial literature, is that the time-varying correlation is adjusted for possible conditional heteroscedasticity. Hence, correcting biased correlations is reduced to break detection in the variance structure. Furthermore, by detecting breaks in the individual parameters, we avoid spurious time varying correlation (Adams et al., 2017) and over-estimation of the persistence in variance and correlation structures (see respectively Hillebrand, 2005 and Aielli, 2013). In addition, we are able to differentiate shifts in the constant correlations from structural changes in the dynamic terms. When the former, a positive change would coincide with a synchronous upward movement, while a negative change may correspond to a *flight-to-quality* dynamic, e.g. risky assets decoupling from safe haven assets (see Baur & Lucey, 2009). When the latter, increased dynamic correlation terms would coincide with the idea that synchronization/decoupling is amplified when innovations take place or with a higher degree of persistence (see Choe et al., 2012).

We apply the $TSSA$ to study contagion between the stock (S) and government bond (B) markets of advanced (AE) and emerging (EME) economies. By doing so, we can make novel conjectures about the way these four markets are interconnected, while most of the empirical studies on contagion are based on one single dimension, i.e. cross-asset or cross-country analysis (Cho et al., 2016).

In the past two decades EME integration to the global financial markets has prompted the development of their S and B markets. However, sudden stops in capital flows posed a significant risk to macroeconomic and financial stability (Sobrun & Turner, 2015). Capital flows are shown to be counter-cyclical in EME (Kaminsky et al., 2004), giving rise to a peculiar relationship between the government bond yields and the earnings of the private companies (Beirne & Gieck, 2014). In addition, changes in the opportunity costs in AE propitiate sudden shifts in the way these markets are interconnected (López & Stracca, 2021). Understanding these dynamics is clue for portfolio rebalancing purposes and to design regulatory policies that promote EME's access to global markets, while restricting contagion risk.

The paper is structured as follows. Section 2 introduces a DCC-GARCH model with possible distinct breaking dates, the test statistics and the $TSSA$. In section 3, we show the results for the Monte Carlo experiments (1) under the assumption of one structural break and (2) by assuming multiple breaks. Section 4 describes the empirical application of the $TSSA$. Concluding remarks are made in Section 5. Finally, the appendix contains complementary tables and figures.

2. Methodology

In this section we propose a methodology to test for the existence of multiple and possible distinct unknown breaks across the covariance parameters of the DCC-GARCH model that employs the $SupLM$ statistic.

The assumption of GARCH processes can reconcile two stylized facts in the literature: (i) time-varying volatility and (ii) time-varying correlations in international asset returns (see Engle, 2002). Moreover, the DCC-GARCH model confers two advantages for the purpose of this paper. Firstly, the GARCH covariance matrix decomposition allows to separately evaluate breaks in the volatility and in the correlation structure. Thus, it enables us to differentiate $shift - contagion$ from increased volatility events. Secondly, following the conditions presented in Engle (2002), the conditional covariance matrices are always positive definite, which ensures the optimization of the log-likelihood functions. Finally, its covariance structure permits to include shocks affecting the level of cross market co-movements, their sensitivity to innovations and persistence.

Under the assumption of multiple unknown breaks, we allow for the possibilities that the breaks are common to a subset of parameters and successive breaks affect different groups of terms. To do so, we propose a three-step segmentation algorithm ($TSSA$). In the first step, we aim to detect multiple breaks occurring in the individual parameters. If two or more parameters appear to present structural shifts, in the second step, we test whether these breaks are common or not. In the last stage, we repeat steps 1 and 2 for the correlation structure given the structural breaks found in the variance terms.

This section is divided in three parts as follows. In the first part we propose a model with possible distinct breaks among all the DCC-GARCH covariance coefficients. For that purpose, as in Perron et al. (2006), we allow successive regimes affecting the individual model parameters. The second part of this section is devoted to compute the test statistic for multiple break detection for each parameter taken one by one. In the first place, we follow Hafner & Herwartz (2008) to derive the score functions of the DCC-GARCH model introduced in Engle (2002). After that, we exhibit the hypothesis testing problems and compute the test statistic. In the third part, we formally present the $TSSA$ when it is applied to the DCC-GARCH model.

2.1. A model with possible distinct breaks

We employ the scalar DCC-GARCH model introduced in Engle (2002). Consider a vector y_t of N assets (market) daily returns for t = 1, . . . , T. The N-dimensional vector is assumed to be normally distributed with zero mean and time-varying covariance Ω_t. Recalling, the covariance matrix can be decomposed like:

$$\Omega_t = V_t R_t V_t,$$

where V_t^2 is a diagonal matrix representing the conditional variance and R_t is the conditional time-varying correlation, symmetric with diagonal entries equal to one.

The statistical specification of the DCC-GARCH model is:

$$V_t^2 = W + A \circ y_{t-1}y'_{t-1} + B \circ V_{t-1}^2,$$

$$\epsilon_t = D_t^{-1} y_t,$$

$$Q_t = \Omega + \alpha\epsilon_{t-1}\epsilon'_{t-1} + \beta Q_{t-1},$$

$$R_t = diag(Q_t)^{-1} Q_t diag(Q_t)^{-1},$$

$$\Omega = R(1 - \alpha - \beta),$$

where $\circ$ corresponds to the hadamard product. The error term (ϵ_t) is volatility-adjusted but still correlated. The variance parameters (W, A and B) are diagonal matrices, the unconditional correlation (R) is symmetric and unit-diagonal, and the dynamic terms of the correlation, α and β, are scalars. For R_t to be positive definite (pd) it suffices that Q_t is pd, which is the case if $\alpha \geq 0$, $\beta \geq 0$, $\alpha + \beta < 1$ and R is pd.

Following Perron et al. (2006), every individual parameter $\psi \in \Psi = [W, A, B, R, \alpha, \beta]$ is subject to a certain number of structural breaks $j_\psi = 1, ..., \lambda_\psi$. Each of these breaks take place at unknown time $T_{\psi,j}$, where the convention that $T_{\psi,0} = 1$ and $T_{\psi,\lambda_\psi+1} = T$ is used.

In order to ensure that the breaking dates are consistently estimated, we impose the assumption proposed in Perron et al. (2006) that the change dates are asymptotically distinct within the individual parameter ψ. To this end, the breaking date is assumed to be located in the position $\pi^*_{\psi,j}$ $\in\Pi \in$ (0,1)[3] of the sample size as follows:

$$T_{\psi,j} = T\pi^*_{\psi,j},$$

where 0< $\pi^*_{\psi,1}$ < $\pi^*_{\psi,2}$<...< $\pi^*_{\psi,\lambda_\psi}$ < 1. Note that, with this condition, when the sample size T increases, all the segments increase in length in the same proportions to each other.

For each break j=1,2,..λ_ψ, the conditional variance can be expressed like :

$$V_t = W + D_{t,\pi^*_{W,j}} \circ \acute{W}_j + A \circ y_{t-1}y'_{t-1} + D_{t,\pi^*_{A,j}} \circ \acute{A}_j \circ y_{t-1}y'_{t-1} + B \circ V^2_{t-1} + D_{t,\pi^*_{B,j}} \circ \acute{B}_j \circ V^2_{t-1},$$

where the dummy variables $D_{t,\pi^*_{\phi,j}}$ are NxN matrices with diagonal entries equal to one when $T_{\psi,j-1} + 1 < t < T_{\psi,j}$.

[3]In the following subsection we define a boundary for this interval, i.e. Π= $[\pi_0$,1 $- \pi_0] \in (0, 1)$ like in Andrews (1993).

Analogously, the conditional correlation is given by:

$$Q_t = (R+R\circ D_{t,\pi^*_{R,j}})(1-\alpha-\beta-(\acute{\alpha}+\acute{\beta})D_{t,\pi^*_{\alpha,\beta,j}})+\alpha\epsilon_{t-1}\epsilon'_{t-1}+\beta Q_{t-1}+(\acute{\alpha}\epsilon_{t-1}\epsilon'_{t-1}+\acute{\beta}Q_{t-1})D_{t,\pi^*_{\alpha,\beta,j}},$$

where $D_{t,\pi^*_{R,j}}$ is a zero matrix whose out-diagonal elements are equal to one when $T_{\psi,j-1}+1 < t < T_{\psi,j}$. Analogously, $D_{t,\pi^*_{\alpha,\beta,j}}$ corresponds to a scalar dummy.

Note that any parameter ψ can present λ_ψ distinct breaks and the break dates $T_{\psi,j}$ are allowed to be distinct or simultaneous among any group of parameters in Ψ.

2.2. Lagrange Multiplier test for unknown multiple breaks in individual parameters

In this subsection we derive the test statistic to allow multiple breaks to take place. We adapt the *SupLM* statistics introduced in Andrews (1993) in order to be able to perform the *repartition* procedure presented in Perron et al. (2006). First, we present the score functions of the DCC-GARCH. Then, we expose the testing problem under the assumption of multiple breaks and proceed to derive the test statistic, i.e., the $SupLM_{\psi,j}$.

2.2.1. The score functions of the DCC-GARCH model

The score functions of the DCC-GARCH, among other multivariate GARCH models, can be found in Hafner & Herwartz (2008). It is worth mentioning that we propose a minor modification of the analytical derivatives reported by the authors. This is, we substitute Ω with $R(1-\alpha-\beta)$ in order to perform the test on the unconditional correlation term R separately form the dynamic parameters α and β. In addition, by taking the assumption that y_t is conditional Gaussian, the information matrix I is equal to the negative expectation of the Hessian matrix J (see Hafner & Herwartz, 2008). However, if desired, the second derivatives can be found in the cited work.

Under the normality assumption the conditional log-likelihood of the observation y (1xN) at time t is maximized by employing the $two-steps$ approach. First, the variance parameters (θ) are estimated. Then, the correlation parameters (ϕ) are estimated with

$\bar{\theta}$ taken as given. For this, the log-likelihood function is decomposed like:

$$l_t(\theta, \phi) = l_t^V(\theta) + l_t^C(\bar{\theta}, \phi),$$

with

$$l_t^V(\theta) = -\frac{1}{2}(Nln2\pi + ln|V_t|^2 + y_t' V_t^{-2} y_t),$$

and

$$l_t^C(\bar{\theta}, \phi) = -\frac{1}{2}(ln|R_t| + \epsilon_t' R_t^{-1} \epsilon_t + \epsilon_t' \epsilon_t).$$

Note that the variance part of the decomposed log-likelihood function is independent of the correlation parameters. While in the correlation part, the variance terms are taken as constants.

The score vector for the volatility part $\frac{\partial l_t^V}{\partial \theta}$ is of length 3N. Then, for the $n-th$ asset we have that:

$$\frac{\partial l_t^V}{\partial \theta_n} = \frac{1}{2v_{n,t}} \frac{\partial v_{n,t}}{\partial \theta_n} (\frac{y_{n,t}^2}{v_{n,t}} - 1),$$

where

$$\frac{\partial v_{n,t}}{\partial \theta_n} = (1, y_{n,t-1}^2, v_{n,t-1}) + b_n \frac{\partial v_{n,t-1}}{\theta_n}.$$

Moreover $v_{n,t}$ and b_n correspond to the $n-th$ diagonal entry of the variance V_t^2 and parameter B matrices respectively.

The score vector for the correlation part $\frac{\partial l_t^C}{\partial \phi}$ is of dimension $(N^* + 2)$, where $N^* = N(N-1)/2$. Thus,

$$\frac{\partial l_t^C}{\partial \phi} = -\frac{1}{2} \frac{\partial vecl(R_t)'}{\partial \phi} vecl[R_t^{-1}(I_N - \epsilon_t \epsilon_t' R_t^{-1})],$$

and

$$\frac{\partial vecl(R_t)'}{\partial \phi} = \frac{\partial vecl(R_t)}{\partial vech(Q_t)'} \frac{\partial vech(Q_t)}{\partial \phi}.$$

Note that, the *vec* operation stack a matrix into a vector, *vech* and *vecl* stack only the lower triangular part of a symmetric matrix, though *vecl* excludes the diagonal. In addition, D_N is the duplication matrix, and $D^+_{N,-}$ its generalized inverse, such that $vec(R) = D_N vecl(R)$ and $vecl(R) = D^+_{N,-} vec(R)$ (see Hafner & Herwartz, 2008 for further details).

For notational simplicity, $Q^*_t = diag(Q_t^{-1/2})$, then:

$$\frac{\partial vecl(R_t)}{\partial vech(Q_t)'} = D^+_{N,-}(Q^*_t \otimes Q^*_t)D_N + D^+_{N,-}(Q_t Q^*_t \otimes I_N + I_N \otimes Q_t Q^*_t)D_N \frac{\partial vech(Q^*_t)}{\partial vech(Q_t)'},$$

where $\otimes$ is the Kronecker product and

$$\frac{\partial vech(Q^*_t)}{\partial vech(Q_t)'} = -\frac{1}{2} diag(vech(Q_t^{-3/2})).$$

Finally, $\frac{\partial vech(Q_t)}{\partial \phi'}$ can be split into the three correlation parameters as follows:

$$\frac{\partial vech(Q_t)}{\partial R'} = \frac{1-\alpha-\beta}{1-\beta} I_d,$$

$$\frac{\partial vech(Q_t)}{\partial \alpha} = -vech(R) + vech(\epsilon_{t-1}\epsilon'_{t-1}) + \beta \frac{\partial vech(Q_{t-1})}{\partial \alpha},$$
$$\frac{\partial vech(Q_t)}{\partial \beta} = -vech(R) + vech(Q_{t-1}) + \beta \frac{\partial vech(Q_{t-1})}{\partial \beta},$$

where I_d is an index matrix which elements take the value of 1 when the corresponding derivative is not null, otherwise zero[4].

[4]E.g. for N=3, $I_d = \begin{Bmatrix} 0 & 1 & 0 & 0 & 0 & 0 & 0 & 0 \\ 0 & 0 & 1 & 0 & 0 & 0 & 0 & 0 \\ 0 & 0 & 0 & 0 & 0 & 1 & 0 & 0 \end{Bmatrix}$.

2.2.2. The testing problem and the test statistic

In order to perform the individual test for multiple breaks, when designing the testing problem, we need first to adopt the assumption of *partial structural change*. For this case, Andrews (1993) defines the subset of coefficients subject to change as ψ_1 such that $\Psi = [\psi_1, \psi_2]$, and ψ_2 is assumed to remain constant. More specifically, ψ_1 contains p parameters and ψ_2 is of length q. In turn, the total number of parameters is $s = p + q$. The methodology employed in the cited work is the partial sample extremum (PSE) estimation. Its main objective is to test for the existence of one breaking date. In practice, the full sample period (t=1...T) can be random uniformly partitioned M times[5] in the interval $\pi \in (\pi_0, 1 - \pi_0)$[6]. However, it is likely to happen that not only one but multiple breaks successively affect ψ_1.

To cover the case of multiple breaks, we perform a bootstrapped *repartition* procedure based on Perron et al. (2006). Its main objective is to test for the existence of some consecutive break j, conditional to the changes pertaining to previous regimes $j - 1$. As follows, to detect any break $j \in 1 : \lambda_\psi$ the length period employed is $\tau_{\psi,j} = T - T_{\psi,j-1} + 1$, with $T_{\psi,0} = 1$. In our case we compute the $SupLM$ with the trimming π_0 applied in the sample period that starts at $T_{\psi,j-1}$ and ends at T.

The testing problem to identify the break $j \in 1 : \lambda_\psi$ is defined as:

$$H_0 : \psi_1(\pi) = \psi_1 \forall t,$$

[5]We propose to define the number of partitions M as 10% of the sample length. See following section for further details.

[6]The authors show that it is necessary to define the first and the last partition sufficiently far away from the first and last data point respectively in order to ensure that the $SupLM$ converges in distribution.

$$H_1 : \psi_1 = \begin{cases} \psi_{1,pre,j}(\pi) = \psi_1, \ \text{for } t \leq T_{\psi,j} \\ \psi_{1,post,j}(\pi) = \psi_1 + \acute{\psi}_1, \ \text{for } t \geq T_{\psi,j}, \end{cases}$$

where $T_{\psi,j-1}$<t<$T_{\psi,j+1}$, $T_{\psi,0} = 1$, $T_{\psi,\lambda_\psi+1} =$ T and π is uniformly distributed in $[\pi_0, 1-\pi_0]$ with length M. Note that π is the point at which the sample is partitioned to detect the true location $\pi^*_{\psi,j}$.

In order to derive the test statistic, we consider the simplified asymptotically equivalent form of the Lagrange multiplier statistic (LM^*) proposed in Andrews & Ploberger (1994). The simplified version is useful for large dimensional models since it employs an information matrix that contains derivatives only with respect to ψ_1. In our case, we need to adapt the LM^* statistic to the *repartition* procedure. In such a way, for the break j and the random partition π, we have that:

$$LM^*_{\psi_1,j}(\pi) = \frac{1}{\sqrt{\tau_{\psi,j}}} \sum_{[T_{\psi,j-1}+\tau_{\psi,j}\pi]}^{T} \frac{\partial l_t(\psi 1, \psi 2)}{\partial \psi_1} \times \left[I_T^{-1}(\pi)_{pre,j} + I_T^{-1}(\pi)_{post,j} \right] \times \frac{1}{\sqrt{\tau_{\psi,j}}} \sum_{[T_{\psi,j-1}+\tau_{\psi,j}\pi]}^{T} \frac{\partial l_t(\psi 1, \psi 2)}{\partial \psi_1},$$

where $T_{\psi,j-1} + \tau_{\psi,j}\pi$ is a random date selected in the sample period that starts as of the previous break until the end of the sample with a trimming at π_0. Note that, under the assumption of one breaking point ($j = 1$), LM^* coincides with the statistic proposed in Andrews & Ploberger (1994) where $T_{\psi,0} + \tau_{\psi,0}\pi = 1 + T\pi$.

Under the assumption of conditional normality of y_t, the Hessian matrix J is equal to the information matrix I. As follows, for every partition π, J is split into *pre* and *post* periods and can be approximated as the sum of the cross products of the first derivatives of log-likehood function (see Hafner & Herwartz, 2008 or Andrews & Ploberger, 1994).

In turn,

$$J_T(\Psi,\pi)_{pre,j} = -\frac{1}{\tau_{\psi,j}} \sum_{T_{\psi,j-1}}^{[T_{\psi,j-1}+\tau_{\psi,j}\pi]} \frac{\partial^2 l_t(\psi 1,\psi 2)}{\partial\psi_1\partial\psi_1} \simeq \frac{1}{\tau_{\psi,j}} \sum_{T_{\psi,j-1}}^{[T_{\psi,j-1}+\tau_{\psi,j}\pi]} \frac{\partial l_t}{\partial\psi_1}\frac{\partial l_t}{\partial\psi_1}',$$

$$J_T(\Psi,\pi)_{post,j} = -\frac{1}{\tau_{\psi,j}} \sum_{[T_{\psi,j-1}+\tau_{\psi,j}\pi]}^{T} \frac{\partial^2 l_t(\psi 1,\psi 2)}{\partial\psi_1\partial\psi_1} \simeq \frac{1}{\tau_{\psi,j}} \sum_{[T_{\psi,j-1}+\tau_{\psi,j}\pi]}^{T} \frac{\partial l_t}{\partial\psi_1}\frac{\partial l_t}{\partial\psi_1}'.$$

The $SupLM_{\psi_1,j}$ is defined as the maximum value of the $LM^*_{\psi_1,j}$ statistic among all the M possible partitions considered. As follows, for successive breaks $j = 1, 2, ..\lambda_\psi$, the pertaining statistic is:

$$SupLM_{\psi_1,j} = Sup_{\pi\in(\pi_0,1-\pi_0)}[LM^*_{\psi_1,j}(\pi)],$$

Note that under the null hypothesis of *no breaking points*, the $SupLM_{\psi_1,j}$ statistic has the same limit distribution as the statistic derived in Andrews (1993). In this way, we are allowed to employ the critical values reported in the cited work. The authors show that its asymptotic null distribution is given by the supremum of the square of a standardized tied-down Bessel process. As follows, they provide the critical values ($qcrit$) for several trimmings (π_0) and numbers of parameters under test (p).

As in Bai (1993) or Galeano & Tsay (2010), the breaking date estimator can be defined as the location where the $SupLM$ is achieved, namely:

$$\widehat{\pi_{\psi_1,j}} = argmax_{\pi_0<\pi<-1-\pi_0} LM^*_{\psi_1,j}(\pi).$$

Finally, we derive the $ExpLM_{\psi_1,j}$ statistic in order to compare its performance with the $SupLM_{\psi_1,j}$. As shown in Andrews & Ploberger (1994), the exponential Lagrange multiplier possess the greatest asymptotic power, however unlike the $SupLM$, it is not able to provide an estimate of the location of the change point (see Galeano & Tsay, 2010). In particular, we choose $ExpLM_{\psi_1,j}(\infty)$ since it gives more weight to alternatives with substantial changes and it is shown to be preferable in terms of power. As follows, the test statistic is given by:

$$ExpLM_{\psi_1,j}(\infty) = log\Big(\frac{1}{\tau_{\psi_1,j}(1-2\pi_0)}\Big[\sum_{[t=T_{\psi,j-1}+\tau_{\psi,j}\pi_0]}^{[T_{\psi,j-1}+\tau_{\psi,j}(\pi_0-1)]} exp(LM^*_{\psi_1,j}(t/\tau_{\psi_1,j})/2)+ \\ exp(LM^*_{\psi_1,j}(\pi_0)/2) + exp(LM^*_{\psi_1,j}(1-\pi_0)/2)\Big]\Big).$$

Analogously, we can employ the asymptotic critical values ($qcrit$) reported in Andrews & Ploberger (1994).

2.3. A three-step segmentation algorithm for detecting multiple and possibly distinct breaks

So far we derived the test statistic to allow for multiple breaks within the group of terms ψ_1. However, there is no a priori reason to believe that only one term would present multiple breaks. Furthermore, in the case that more than one parameter is affected, then, the changes might not be common to all the terms. For example, it could be the case that after a common break in the parameters A and B, a second structural change affects only A. In this sense, our three-step segmentation algorithm ($TSSA$) can detect multiple and possibly distinct breaks that may take place among some or all the covariance parameters. In the first step, the algorithm aims to detect sequential breaks affecting each individual parameter by performing a bootstrapped *repartition* procedure based on Perron et al. (2006). In the second step, a *distinctiveness* detection is employed to determine whether the identified breaks lie close to each other. The last steps is aimed to find breaks in the correlation structure, given the breaks found in the variance terms.

We base our *distinctiveness* detection step on the test introduced in Oka & Perron (2018). However, we follow Blatt et al. (2015) to design the procedure. As noticed by the authors, the test offers no rule to differentiate dates lying *close together*. Consequently, they encourage the testing whenever the confidence intervals of the estimated breakpoints overlap. It is worth to note that, since the authors employ the LR statistic, they need to compute the estimates under the null (*all breaks are simultaneous*) and under the alternative (*at least one break is distinct*). By contrast, the LM statistic only makes use of the estimated parameters of the restricted model. As follows, under the assumption of asymptotically distinct breaks affecting the individual parameters as in Perron et al., 2006) and the null hypothesis of *all simultaneous breaks*, within each regime, the estimates have the same limit distributions as under the null of *no changes*.

We propose a bootstrapped *repartition* procedure of L repetitions (with L sufficiently large, e.g. L=1,000). More specifically, we replicate L times M random variables uniformly distributed in $\pi \in (\pi_0, 1-\pi_0)$ and compute the $LM^*_{\psi,j}(\pi)^l$ statistic in each sample partition (π) and replication (l)[7]. By doing so, we extend the search over many possible combinations of break locations for each replication of the simulations. As follows we take the sequence $(\widehat{\pi_{\psi,j}}^l)_{l\in P\subset L}$ composed by the estimated break positions obtained in the $P \subset L$ replications for which a break is detected, i.e., $SupLM^l_{\psi,j} > qcrit$. Note that, $\frac{P}{L}$ can be interpreted as a measure of the power of the break detection j in ψ. Furthermore, we define $\wp$ as a desired (non-trivial) power. If a break is detected an amount of times sufficiently large among the L replications ($\frac{P}{L} > \wp$) for more than one parameter, in a second stage, we intent to determine whether the detected changes are significantly distinct among the affected terms.

In order to proceed with the *distinctiveness* detection, we first take the estimated break positions $(\widehat{\pi_{\psi,j}}^l)_{l\in P}$ when $\frac{P}{L} > \wp$. Then, as in Oka & Perron (2018), we collect

[7] To simplify the notation we drop the subscript in ψ_1, hereafter ψ denotes the individual parameter under test.

their corresponding pairs $(\psi, j) \subseteq (1, ..., s) \times (1, ..., \lambda_\psi)$. As follows, we compute the total number of identified breaks, $\lambda_{total} = \sum_\psi \lambda_\psi$, to define the maximum amount of possible distinct breaks. Thus, we create G disjoint sets of pairs (ψ, j), $\mathcal{G}_1, \mathcal{G}_2, ..., \mathcal{G}_G \subseteq \{(1, .., s) \times (1, .., \lambda_{total}\}$, such that within each group, $\mathcal{G}_g$, all the parameters share the same break dates. Consequently, the distinct break dates are denoted as T_g, where $g = 1, ..., G$.

With the purpose of creating the sets $\mathcal{G}_g$, we proceed as in Blatt et al. (2015). First, we construct 95% confidence $(CI_{\psi,j})$ of the estimated break positions $(\widehat{\pi_{\psi,j}}^l)_{l \in P}$ for all ψ and j for which $\frac{P}{L} > \wp$. If none $CI_{\psi,j}$ overlaps, each group $\mathcal{G}_g$ is composed by one single pair (ψ, j). If two or more $CI_{\psi,j}$ overlap, we cluster the corresponding pairs (ψ, j) in the same set $\mathcal{G}_g$. Note that the amount of groups G is zero when any shift is detected and achieves its maximum at λ_{total} when all the breaks are distinct. On the other hand, when all the parameters share the same dates, it has to be the case that the amount of detected breaks are equal for all ψ and, thus, $G = \lambda_\psi$. Finally, the estimated distinct breaks $\widehat{\psi_g}$ are computed as the average of the $CI_{\psi,j}$ between the pairs (ψ, j) that belong to the same group g.

In the last step, we detect structural changes occurring in the correlation structure by employing the stacked time-varying volatility within the regimes found in the previous two steps. Let us assume that we found G_θ distinct changes affecting the variance structure and that the estimated variance parameters within these regimes are $\bar{\theta} = [\theta_1, \theta_2, ...\theta_{G_\theta}]$. As follows, we repeat steps 1 and 2 of the $TSSA$ for the the correlation parameters (ϕ) by employing the stacked volatility in the second stage DCC-GARCH estimation procedure. Recalling, in this second stage the likelihood function is given by $l_t^C(\bar{\theta}, \phi)$. As a result, we correct the bias on the estimated correlation parameters due to shifts occurring in the variance structure.

The formal three-step segmentation algorithm $(TSSA)$ proceeds as follows:

1. Replicate L times the *repartition* procedure for every single parameter $\psi \subseteq \Psi$:

   (a) Create L sorted random variables, $\pi_{\psi}^{l} \in \mathbb{R}^{M}$, distributed within the interval $[\tau_{\psi,j-1}\pi_0, \tau_{\psi,j-1}(1-\pi_0)]$ where $\tau_{\psi,0} = T$, $m \in (0,1)$, $M = m\tau_{\psi,j-1}$, $\pi_0 \in (0,1/2)$, $l \in [1,..,L]$ and L is sufficiently large.

   (b) Compute $SupLM_{\psi,j}^{l}$ for all $l \in [1,...,L]$:

      i. If $SupLM_{\psi,j}^{l} > qcrit$ for all $l \in [1,...,P]$ but $\frac{P}{L} < \wp$, the detection is terminated.

      ii. If $SupLM_{\psi,j}^{l} > qcrit$ all $l \in [1,...,P]$ but $\frac{P}{L} \geq \wp$, retrieve the breaking date estimators $\widehat{\pi_{\psi,j}}^{l}$ and compute $\tau_{\psi,j}^{l} = T - \widehat{\pi_{\psi,j}}^{l} T$. Repeat steps $1.a$ and $1.b$ until the detection is terminated or until $\tau_{\psi,j}^{l}\pi_0$ is close to T[8].

2. Determine whether the estimated break positions found in previous step (if any) are significantly distinct among the different parameters.

   (a) Take the sequences $(\widehat{\pi_{\psi,j}}^{l})_{l \in P}$ for every pair (ψ, j) for which $\frac{P}{L} > \wp$. Sort the sequences and compute the 95% confidence intervals $(CI_{\psi,j})$.

   (b) For each $CI_{\psi,j}$ collect the pairs $(\psi, j) \subseteq (1,...,s) \times (1,...,\lambda_{\psi})$. Then, take all possible combinations of 2,...,λ_{total} collected pairs for distinct ψ's. If for a given combination:

      i. the confidence intervals overlap, take the corresponding pairs and create the group $\mathcal{G}_g$.

      ii. the confidence intervals do not overlap, create the groups $\mathcal{G}_g$ conformed by the corresponding single pairs.

   (c) Compute $\widehat{\pi_g} = \underset{(\psi,j) \in \mathcal{G}_g}{Avg} (CI_{\psi,j})$ for all the sets $\mathcal{G}_g$ defined in previous step.

[8] With $T - \tau_{\psi,j}^{l}\pi_0 > 100$ the DCC-GARCH estimation normally converges.

3. Estimate the variance parameters $\bar{\theta} = [\theta_1, \theta_2, ...\theta_{G_\theta}]$ within the G_θ distinct dates found in the previous steps and repeat steps 1 and 2 for the correlation parameters (ϕ) using the log-likelihood function $l_t^C(\bar{\theta}, \phi)$.

3. Monte Carlo Experiments

We conduct five Monte Carlo experiments that can be divided in two groups. The first group is aimed to analyze the performance of the $SupLM$ when detecting structural breaks affecting the covariance parameters of the DCC-GARCH model one by one under the assumption of one unknown breaking point. The second group of experiments is oriented to analyze the accuracy of the $TSSA$ under the assumption of multiple breaks. More specifically, the last group considers: (1) two successive breaks affecting each term of the covariance structure one by one and (2) two successive breaks assigned, first, to the variance and then, to the correlation structure.

We simulate $1,000$ series under the null of no-change and other $1,000$ under the alternative. We choose the coefficients of the DCC-GARCH model such that the condition of a *pd* conditional covariance matrix is ensured in the process of optimisation. The parameter values employed to simulate the series under the null and the alternative hypothesis for each experiment are reported in the Appendix, Table 7. The first four experiments are performed with the same changes in parameters, while the last experiment conducts smaller changes in order to preserve the *pd* conditions. The difference relies on the fact that the first four experiments simulate the break(s) in each parameter taken one by one, and thus larger changes in the terms are allowed. This is, we simulate a break affecting only one parameter while the rest remains unchanged[9]. In the last

[9]In order two simplify the exposition of result, when testing the dynamic terms of the correlation structure we simulate a simultaneous break in both terms and we stack the two score functions, thus only simultaneous breaks occurring in α and β are detected. This approach can be easily lifted by

experiment, we simulate a change in all the variance, and later on in the correlation structure, thus the simultaneous changes have to satisfy the *pd* conditions.

In all the cases we compute the size and the size-adjusted power and we measure the ability of the breaking date estimator to detect the location of the true shift point(s). For the size, we retrieve the critical values reported in Andrews (2003) and Andrews & Ploberger (1994) at 5% of significance for the $SupLM$ and $ExpLM$ statistics respectively. The size is computed as the percentage of the sorted sequence whose elements are larger than the corresponding critical values, where the sequences $(SupLM^{l}_{\psi,j})_{(l\in L)}$ and $(ExpLM^{l}_{\psi,j})_{(l\in L)}$ are computed under H0. For the size-adjusted power, we first retrieve the value of the sorted sequences under H0 at the 95% quantiles (denoted in the tables as $SupLM_{0.95}$ and $ExpLM_{0.95}$). As follows, we sort the analogous sequences under H1 and calculate the percentage of their elements that are higher than the corresponding 95% quantiles. We also employ these sequences created under the alternative to construct the 95% confidence intervals $(CI_{\psi,j})$ needed for the *distinctiveness* test step. Finally, we compute the mean, min, max and standard deviation of the $(CI_{\psi,j})$.

The results of the experiments are disclosed in the Tables 1 to 5 reported in this section. The Appendix contains the figures where we show the probability density of the test statistics for the experiment (i) and the ability of the $TSSA$ to detect the position of the true breaking point(s) when the experiment (iv) and (v) are performed (see respectively Figures 1 to 4.

3.1. Under the assumption of one breaking point

Under the assumption of one breaking point, we measure the performance of the $SupLM$ and the $ExpLM$ and compare their size and power among three experiments: (i) a small, medium and large changes affecting each parameter one by one, (ii) the true

considering each score function individually.

breaking point located in the extremes of the sample and (iii) the size of the portfolio varies. In particular, the first experiment is aimed to disclose whether the $SupLM$, as proposed in Andrews (1993), has monotonic power when it is applied to the DCC-GARCH framework. In this sense, Vogelsang (1999) suggested that the $SupLM$ statistic may present the problem of non monotonic power i.e. for a fixed sample, its power tends to zero as the change in mean parameters increases.

Table 1 reports the first experiment where three assets and three different sample sizes $T = [500, 700, 1, 000]$ are considered. Under the alternative, the true breaking point is located in the middle of the sample ($\pi^*_{\psi,1} = 0.5$) and we simulate a small, a medium and a large structural change (see values in Table 7).

We can note that the size decreases and the power increases monotonically. The maximum size obtained is 0.100 observed at $T = 500$ for the test on $[\alpha, \beta]$. However, for $T = 1, 000$, the size decreases to 0.08. The power monotonically increases as $T \to \infty$ and for larger changes on the parameters in all the cases. The $CI_{\psi,j}$'s include the true breaking points $\pi^*_{\psi,1}T$. We observe also decreasing error days when the percentage change of the parameters increases.

In Figures 1 and 2 we report the probability density of the sequences $(SupLM^l_{\psi,j})_{(l\in L)}$, under the null and the alternative hypothesis, for small, medium and large changes of the parameters. We observe that, after the critical values ($qcrit$), the probability density under the null decreases as $T \to \infty$. On the other hand, under the alternatives, the probability densities are accumulated further away from $SupLM_{0.95}$ as $T \to \infty$ and larger changes are applied to the parameters.

Table 2 reports the results of the second experiment when the true breaking point is located close to the beginning ($\pi^*_{\psi,1}$=0.3), in the middle ($\pi^*_{\psi,1}$=0.5) or near the end of the sample ($\pi^*_{\psi,1}$=0.7). By considering three assets, we compute a large change on each parameter taken one by one under the alternative. From the results, we can infer that the power almost does not change when the breaking point is still located within the

Table 1: (i) experiment: small, medium and large changes affecting each parameter one by one

Test	W			A			B			R			α and β		
T	500	700	1,000	500	700	1,000	500	700	1,000	500	700	1,000	500	700	1,000
$\pi^*_{\psi,1}T$	250	350	500	250	350	500	250	350	500	250	350	500	250	350	500
SIZE															
SupLM															
size[1]	0.06	0.05	0.05	0.12	0.09	0.08	0.08	0.05	0.05	0.04	0.03	0.03	0.10	0.09	0.08
$\text{SupLM}_{0.95}$	13.84	12.81	12.89	16.13	14.94	14.46	14.35	13.05	13.06	12.09	12.32	12.44	13.22	13.58	12.33
ExpLM															
size[2]	0.02	0.02	0.01	0.05	0.03	0.03	0.02	0.02	0.02	0.01	0.01	0.01	0.05	0.04	0.03
$\text{ExpLM}_{0.95}$	3.02	2.56	2.55	4.27	3.53	3.09	3.31	2.65	2.83	2.49	2.51	2.56	2.96	2.93	2.44
POWER															
SMALL															
SupLM															
power	0.76	0.92	0.98	0.45	0.58	0.76	0.72	0.89	0.98	0.39	0.58	0.73	0.31	0.42	0.47
mean	229	330	477	232	328	476	233	333	479	241	333	480	211	305	444
min	131	204	351	131	197	285	140	210	351	140	210	300	128	180	257
max	282	395	536	322	428	629	288	407	552	330	426	596	332	453	681
sd	151	191	185	191	231	344	148	197	201	190	216	296	204	273	424
ExpLM															
power	0.77	0.92	0.99	0.31	0.58	0.75	0.69	0.89	0.98	0.58	0.59	0.84	0.22	0.42	0.43
MEDIUM															
SupLM															
power	1.00	1.00	1.00	0.96	0.99	1.00	1.00	1.00	1.00	0.56	0.72	0.78	0.44	0.56	0.62
mean	241	338	490	243	341	489	243	342	493	236	321	456	214	309	433
min	178	278	440	169	249	397	210	308	467	140	200	285	128	180	257
max	263	360	515	290	385	536	257	350	500	306	401	536	330	453	664
sd	85	82	75	121	136	139	47	42	33	166	201	251	202	273	407
ExpLM															
power	1.00	1.00	1.00	0.91	0.99	1.00	1.00	1.00	1.00	0.74	0.85	0.88	0.34	0.46	0.58
LARGE															
SupLM															
power	1.00	1.00	1.00	1.00	1.00	1.00	1.00	1.00	1.00	0.68	0.77	0.82	0.53	0.65	0.71
mean	242	341	492	245	343	493	242	339	490	226	308	435	210	303	435
min	192	294	455	191	291	436	210	294	456	131	183	262	128	180	257
max	257	357	509	275	375	527	250	350	500	282	369	509	332	462	660
sd	65	63	54	84	84	91	40	56	44	151	186	247	204	282	403
ExpLM															
power	1.00	1.00	1.00	0.99	1.00	1.00	1.00	1.00	1.00	0.83	0.88	0.90	0.44	0.57	0.68

Notes:
(1) Critical values retrieved from Andrews (2003) for $\alpha = 0.05$, $\pi_0 = 0.25$, (2) critical values retrieved from Andrews and Ploberger (1994) for $\alpha = 0.05$, $\pi_0 = 0.25$ and $c = \infty$,(3) $SupLM_{0.95}$ and $ExpLM_{0.95}$ are the 95-percentile of the corresponding LM statistics, (4) mean, min, max and sd are statistics retrieved from the 95% confidence intervals of the SupLM statistics, (5) N=3, (6) SMALL, MEDIUM and LARGE correspond respectively to percentage changes on W,A,B: (+50%, +100%, +125%), R: (+200%, +250%, +300%) and α and β: (+500%, +600%,+700%).

boundary $\Pi = (0.25, 0.75)$. These results coincide with Andrews (1993) who suggested that, when π lays on some restricted interval bounded away from 0 and 1 (Π), the test statistic maximizes its power.

Table 3 shows the performance of the tests when two, three and four assets are considered. In order to simplify the exposition of results, under the alternative, we perform a large change located in the middle of the sample affecting each parameter one by one. We observe that the power decreases when the dimension of the portfolio

Table 2: (ii) experiment: π^* located in the extremes of the sample

Test		W			A			B			R			α and β	
T	500	500	500	500	500	500	500	500	500	500	500	500	500	500	500
$\pi^*_{\psi,1}T$	150	250	350	150	250	350	150	250	350	150	250	350	150	250	350
SIZE															
SupLM															
size[1]	0.06	0.06	0.06	0.12	0.12	0.12	0.08	0.08	0.08	0.04	0.04	0.04	0.10	0.10	0.10
$\text{SupLM}_{0.95}$	13.84	13.84	13.84	16.13	16.13	16.13	14.35	14.35	14.35	12.09	12.09	12.09	13.22	13.22	13.22
ExpLM															
size[2]	0.02	0.02	0.02	0.05	0.05	0.05	0.02	0.02	0.02	0.01	0.01	0.01	0.05	0.05	0.05
$\text{ExpLM}_{0.95}$	3.02	3.02	2.99	4.27	4.25	4.20	3.31	3.33	3.30	2.49	2.50	2.49	2.96	3.00	2.97
POWER															
LARGE															
SupLM															
power	1.00	1.00	0.99	1.00	1.00	0.98	1.00	1.00	1.00	0.60	0.68	0.73	0.57	0.53	0.50
mean	149	242	332	155	245	330	147	242	338	155	226	323	166	210	288
min	131	192	257	131	191	228	131	210	297	128	131	178	128	128	128
max	169	257	352	192	275	361	150	250	350	210	282	359	275	332	361
sd	38	65	95	61	84	133	19	40	53	82	151	181	147	204	233
ExpLM															
power	1.00	1.00	0.99	0.96	0.99	0.97	1.00	1.00	1.00	0.68	0.83	0.86	0.45	0.44	0.39

Notes:
(1) Critical values retrieved from Andrews (2003) for $\alpha = 0.05$, $\pi_0 = 0.25$, (2) critical values retrieved from Andrews and Ploberger (1994) for $\alpha = 0.05$, $\pi_0 = 0.25$ and $c = \infty$,(3) $SupLM_{0.95}$ and $ExpLM_{0.95}$ are the 95-percentile of the corresponding LM statistics, (4) mean, min, max and sd are statistics retrieved from the 95% confidence intervals of the SupLM statistics, (5) N=3, (6) LARGE corresponds to percentage change on W,A,B: (+125%), R: (+300%) and α and β: (+700%).

increases, except for the scalars α and β. This result can be related to the fact that the estimation of the covariance parameters becomes more challenging when the dimension becomes larger relatively to the sample size (see Engle, 2009). The exception is for α and β parameters, which have always the same dimension no matter how big the system is.

3.2. Under the assumption of multiple breaking points

In this subsection, we remove the assumption of $j = 1$ and we test the performance of the $TSSA$. To this end, we conduct the experiments (iv) two successive breaks affecting each term of the covariance structure one by one and (v) two successive breaks assigned, first, to the variance and then, to the correlation structure.

Hereinafter, we refer to *rounds* to each sample period that starts as of the last break point detected, with the first round starting at the t=1. Thus, the round o covers the sample period from $T_{\psi,o-1}$ to T, with $T_{\psi,0} = 1$ and $T_{\psi,o} = \widehat{\pi_{\psi,o}}T$. For ease of exposition, we assume a maximum or three rounds (o=1,2,3).

Table 3: (iii) experiment: the size of the portfolio varies

Test	W			A			B			R			α and β		
T	500	500	500	500	500	500	500	500	500	500	500	500	500	500	500
$\pi^*_{\psi,1}T$	250	250	250	250	250	250	250	250	250	250	250	250	250	250	250
N	2	3	4	2	3	4	2	3	4	2	3	4	2	3	4
SIZE															
SupLM															
size	0.07	0.06	0.02	0.14	0.12	0.04	0.08	0.08	0.01	0.04	0.04	0.01	0.09	0.10	0.07
$\mathrm{SupLM}_{0.95}$	16.39	13.84	7.90	18.73	16.13	9.90	16.90	14.35	8.11	18.15	12.09	5.72	14.27	13.22	12.09
ExpLM															
size	0.02	0.02	0.01	0.05	0.05	0.01	0.03	0.02	0.00	0.01	0.01	0.01	0.05	0.05	0.04
$\mathrm{ExpLM}_{0.95}$	4.13	3.02	0.57	5.17	4.27	1.28	4.32	3.31	0.51	5.32	2.49	0.08	3.63	2.96	2.29
POWER															
LARGE															
SupLM															
power	1.00	1.00	0.72	1.00	1.00	0.66	1.00	1.00	0.64	0.90	0.68	0.56	0.45	0.53	0.44
mean	244	242	234	245	245	243	244	242	232	237	226	214	262	210	205
min	210	192	156	192	191	152	218	210	156	156	131	128	128	128	128
max	257	257	275	268	275	308	250	250	250	275	282	322	352	332	288
sd	47	65	119	76	84	156	32	40	94	119	151	194	224	204	160
ExpLM															
power	1.00	1.00	0.87	1.00	0.99	0.77	1.00	1.00	0.93	0.95	0.83	0.67	0.39	0.44	0.38

Notes:
(1) Critical values retrieved from Andrews (2003) for $\alpha = 0.05$, $\pi_0 = 0.25$, (2) critical values retrieved from Andrews and Ploberger (1994) for $\alpha = 0.05$, $\pi_0 = 0.25$ and $c = \infty$,(3) $SupLM_{0.95}$ and $ExpLM_{0.95}$ are the 95-percentile of the corresponding LM statistics, (4) mean, min, max and sd are statistics retrieved from the 95% confidence intervals of the SupLM statistics, (5) π^*=0.5, (6) LARGE corresponds to percentage change on W,A,B: (+125%), R: (+300%) and α and β: (+700%).

In the experiment (iv), we simulate two breaking points under the alternative. More specifically, we locate the two breaks at $\pi^*_{\psi,j=1} = 0.30$ and $\pi^*_{\psi,j=2} = 0.70$. After the first break, we perform a large change in the corresponding parameters. From the second one to the end of the sample, we employ the parameter values under H0.[10]

Figure 3 illustrates the probability density functions for the estimated breaking points for 1,000 simulations and T=1,000. The blue density function exhibits the location of the estimated breaks under H0. We can notice that, reflecting trivial size, the blue line is in almost all the cases close to the x-axis, implying that the $TSSA$ do not detect fake breaks despite that the sample period shrinks. The three red densities denote the estimated locations found under the alternative hypothesis in the first (dark red), the second (red) and the third (light red) round. We observe that the first round concentrates the location

[10] In order to stack the series, the simulations consider the initial values of the covariance matrix as the last estimated values obtained from the previous regime.

of the estimated breaks close to $\pi^*_{\psi,1}$ and $\pi^*_{\psi,2}$. The second round is concentrated around $\pi^*_{\psi,2}$ while during the third one almost any break is detected.

As can be noticed in the Figure 3 the first round is capturing sometimes the first and sometimes the second true breaking point. Thus, by taking the average of the estimated positions in the first round, we would obtained an estimated location between $\pi^*_{\psi,1}$ and $\pi^*_{\psi,2}$. In order to increase the accuracy of the estimated mean positions we implement the k-mean clustering algorithm introduced in Hartigan & Wong (1979). We first take the sequences of the estimated changing positions, $(\widehat{\pi_{\psi,o}}^l)_{l\in P}$, for which $\frac{P}{L} > \wp$, with the total amount of observations that satisfies this condition among all the rounds being P_{total}[11]. As follows, we perform the k-mean clustering along these P_{total} observations and conform three groups ($k = 1, 2, 3$). If one group contains less than 5% of the total observations, we drop it and repeat the k-mean clustering with one group less. We keep on dropping groups until all the clusters contain more than 5% of the observations. We compute the 95% confidence intervals per cluster and their corresponding mean, minimum, maximum and standard deviation. Finally, we account for the percentage of the power ($\%power_k$) that each group represents, i.e. the number of positions concentrated around the mean of a k-group divided by the total amount of positions where a break was detected.

Table 4 shows that the first and the second round present non-trivial power and the true breaking positions are within the $CI_{\psi,o}$'s. Accurately, in the third round almost any changing point is found. When applying the k-mean clustering, the estimated mean positions are closer to the true breaking points for the groups that concentrate the larger power ($\%power$). For example, for the constant correlation term R and $T = 500$, the first and third groups concentrate, respectively, the 42% and the 41% of the power, with $CI\psi, o$'s containing the true breaking points and standard deviations no longer than 13

[11]Recalling, P is the subset of L replications for which $SupLM^l_{\psi,o} > qcrit$.

days. Conversely, only 17% of the observations lay in the interval [215,290] that does not contain any true braking point.

Table 4: (iv) experiment: two successive breaks affecting each parameter one by one

Test	W			A			B			R			α and β		
T	500	700	1,000	500	700	1,000	500	700	1,000	500	700	1,000	500	700	1,000
$\pi^*_{\psi_1,1}T$	150	210	300	150	210	300	150	210	300	150	210	300	150	210	300
$\pi^*_{\psi_1,2}T$	350	490	700	350	490	700	350	490	700	350	490	700	350	490	700
SIZE															
o=1															
size	0.07	0.05	0.05	0.12	0.09	0.08	0.08	0.04	0.05	0.03	0.04	0.03	0.09	0.09	0.08
$ExpLM_{0.95}$	13.90	12.87	13.46	16.36	14.73	14.76	14.39	12.94	13.25	12.01	12.40	12.21	13.11	13.91	12.47
o=2															
size	0.01	0.00	0.00	0.02	0.01	0.01	0.02	0.00	0.00	0.00	0.00	0.00	0.03	0.04	0.02
$ExpLM_{0.95}$	11.93	11.32	11.19	12.39	11.85	11.81	12.13	11.82	11.17	11.16	10.99	11.18	10.26	10.33	10.02
o=3															
size	0.00	0.00	0.00	0.01	0.00	0.00	0.01	0.00	0.00	0.00	0.00	0.00	0.02	0.02	0.01
$ExpLM_{0.95}$	11.88	11.18	11.14	12.10	11.82	11.72	12.00	11.77	11.14	11.16	10.99	11.17	10.08	9.91	9.90
POWER															
o=1															
power	0.87	0.98	1.00	0.92	0.99	1.00	0.95	0.99	1.00	0.63	0.99	0.76	0.88	0.99	0.96
mean	246	348	495	253	350	506	252	368	521	183	201	405	194	196	384
min	129	183	265	131	184	267	131	184	267	126	175	252	126	175	251
max	369	516	735	366	513	729	354	495	706	348	287	699	349	274	700
sd	240	333	470	235	329	462	223	311	439	222	112	447	223	99	449
o=2															
power	0.48	0.54	0.56	0.48	0.56	0.55	0.48	0.46	0.48	0.33	0.94	0.43	0.60	0.83	0.71
mean	361	504	718	360	505	717	354	499	712	302	352	633	297	356	617
min	332	474	685	310	449	651	330	468	674	226	308	455	224	308	447
max	418	574	818	443	610	866	416	594	849	357	485	712	386	487	737
sd	86	100	133	133	161	215	86	126	175	131	177	257	162	179	290
o=3															
power	0.05	0.05	0.06	-	0.06	0.06	-	0.04	0.05	0.15	0.78	0.13	0.33	0.61	0.36
mean	-	589	834	-	598	850	-	592	853	343	454	692	345	458	700
min	-	544	775	-	543	756	-	549	776	302	410	600	298	409	596
max	-	651	922	-	650	940	-	651	940	391	516	808	418	544	843
sd	-	107	147	-	107	184	-	102	164	89	106	208	120	135	247
K-mean															
k=1															
$\%power_{k=1}$	0.32	0.31	0.31	0.30	0.30	0.30	0.30	0.28	0.28	0.42	0.37	0.35	0.33	0.38	0.33
mean	143	201	288	147	204	293	142	200	288	137	185	272	139	183	275
min	127	180	258	128	180	258	128	180	259	126	175	251	126	175	251
max	156	216	305	177	233	321	150	210	300	154	240	355	168	222	360
sd	7	10	12	10	11	13	6	9	11	8	12	19	10	8	25
k=2															
$\%power_{k=2}$	0.64	0.65	0.65	0.66	0.66	0.66	0.67	0.70	0.69	0.17	0.18	0.18	0.22	0.29	0.19
mean	356	497	709	352	495	705	348	489	699	248	280	474	249	323	489
min	336	477	687	316	456	660	331	471	680	215	277	384	213	291	398
max	404	554	782	410	570	812	389	548	754	290	296	567	291	370	586
sd	13	14	17	17	21	23	8	10	10	20	19	49	21	16	47
k=3															
$\%power_{k=3}$	-	-	-	-	-	-	-	-	-	0.41	0.45	0.47	0.45	0.33	0.49
mean	-	-	-	-	-	-	-	-	-	341	452	687	341	455	692
min	-	-	-	-	-	-	-	-	-	305	407	609	303	407	614
max	-	-	-	-	-	-	-	-	-	371	513	727	402	542	794
sd	-	-	-	-	-	-	-	-	-	13	29	41	20	34	45

Notes:
(1) Critical values retrieved from Andrews (2003) for $\alpha = 0.05$, $\pi_0 = 0.25$ (2) $SupLM_{0.95}$ is the 95-percentile of the SupLM statistics, (3) mean, min, max and sd are statistics retrieved from the 95% confidence intervals of the SupLM statistics, (4) K-mean re-groups the SupLM statistics obtained when combining all rounds in max 3 clusters, power, mean, min, max and sd are retrieved from the clusters, (5) N=3, (6) percentage change on W,A,B: (+20%), R: (+300%) and α and β: (+700%).

The last experiment covers the case for which the variance and correlation structures are affected by two successive structural breaks, respectively $\pi^*_{\theta,1} = 0.3$ and $\pi^*_{\phi,1} = 0.7$. As can be observed in the Figure 4, the first round concentrates the location of the estimated breaking points close to the true positions in all the tests for T=1,000. For different sample sizes, Table 5 shows that, for the variance parameters, the first round presents non-trivial power and $CI_{\psi,o=1}$ includes the true breaking point. In addition, when applying the k-mean algorithm, two groups are dropped since they represent less than 5% of the positions where a break is detected. For the correlation structure, the table reports that the three rounds lie close to each other, whereas the estimated mean position obtained after the k-mean clustering gives more precise dates. The second group (k=2) represents around 50% of the observations, with $CI_{\psi,k=2}$ including the true locations and standard deviations below 20 days in all the cases.

Table 5: (v) experiment: two successive breaks affecting $\theta = [W, A, B]$ ($\pi_1 = 0.3$) and $\phi = [R, \alpha, \beta]$ ($\pi_1 = 0.7$)

Test	W			A			B			R			α and β		
T	500	700	1,000	500	700	1,000	500	700	1,000	500	700	1,000	500	700	1,000
$\pi^*_{\psi_1,1}T$	150	210	300	150	210	300	150	210	300	350	490	700	350	490	700
SIZE															
o=1															
size	0.07	0.05	0.05	0.12	0.09	0.08	0.08	0.04	0.05	0.03	0.04	0.03	0.09	0.09	0.08
$\text{ExpLM}_{0.95}$	13.90	12.87	13.46	16.36	14.73	14.76	14.39	12.94	13.25	12.01	12.40	12.21	13.11	13.91	12.47
o=2															
size	0.01	0.00	0.00	0.02	0.01	0.01	0.02	0.00	0.00	0.00	0.00	0.00	0.03	0.04	0.02
$\text{ExpLM}_{0.95}$	11.93	11.32	11.19	12.39	11.85	11.81	12.13	11.82	11.17	11.16	10.99	11.18	10.26	10.33	10.02
o=3															
size	0.00	0.00	0.00	0.01	0.00	0.00	0.01	0.00	0.00	0.00	0.00	0.00	0.02	0.02	0.01
$\text{ExpLM}_{0.95}$	11.88	11.18	11.14	12.10	11.82	11.72	12.00	11.77	11.14	11.16	10.99	11.17	10.08	9.91	9.90
POWER															
o=1															
power	0.65	0.82	0.95	0.65	0.79	0.91	0.70	0.85	0.96	1.00	1.00	1.00	1.00	1.00	1.00
mean	154	215	303	162	220	307	156	216	302	302	425	608	246	361	528
min	128	179	256	129	180	257	128	180	257	277	405	585	127	177	253
max	198	277	374	236	302	388	206	275	366	342	463	654	318	443	623
sd	70	98	118	107	122	131	78	95	109	65	58	69	191	266	370
o=2															
power	0.04	0.04	0.05	0.06	0.08	0.08	0.06	0.06	0.06	0.58	0.60	0.60	0.69	0.66	0.63
mean	331	499	733	356	498	691	347	492	715	366	514	735	323	464	673
min	225	349	485	244	357	497	234	328	497	331	485	696	228	319	475
max	414	577	825	422	585	818	419	576	823	425	580	840	388	555	786
sd	189	228	340	178	228	321	185	248	326	94	95	144	160	236	311
o=3															
power	0.00	0.01	0.01	0.01	0.01	0.01	0.01	0.01	0.00	0.36	0.39	0.40	0.42	0.42	0.39
mean	351	578	874	422	611	855	412	602	914	403	570	816	376	532	776
min	328	466	814	316	519	829	358	466	874	372	542	775	303	423	619
max	368	621	947	470	649	893	471	641	947	435	624	911	425	610	874
sd	40	155	133	154	130	64	113	175	73	63	82	136	122	187	255
K-mean															
k=1															
$\%\text{power}_{k=1}$	0.99	0.99	0.98	0.97	0.99	0.99	0.99	0.99	0.99	0.18	0.18	0.17	0.16	0.13	0.11
mean	151	211	299	157	215	303	153	212	299	301	423	604	136	187	262
min	128	180	257	129	180	257	128	181	257	263	403	584	125	175	251
max	198	276	374	233	301	384	206	275	365	320	450	638	171	220	297
sd	15	20	22	22	24	25	16	20	21	9	9	11	10	11	10
k=2															
$\%\text{power}_{k=2}$	-	-	-	-	-	-	-	-	-	0.48	0.48	0.48	0.50	0.51	0.51
mean	-	-	-	-	-	-	-	-	-	358	503	715	353	493	698
min	-	-	-	-	-	-	-	-	-	331	477	687	321	488	675
max	-	-	-	-	-	-	-	-	-	377	529	751	389	529	753
sd	-	-	-	-	-	-	-	-	-	10	12	14	18	19	13
k=3															
$\%\text{power}_{k=3}$	-	-	-	-	-	-	-	-	-	0.34	0.34	0.35	0.34	0.37	0.38
mean	-	-	-	-	-	-	-	-	-	407	570	813	375	526	751
min	-	-	-	-	-	-	-	-	-	386	543	774	345	484	695
max	-	-	-	-	-	-	-	-	-	442	625	904	420	598	861
sd	-	-	-	-	-	-	-	-	-	13	20	32	22	31	44

Notes:
(1) Critical values retrieved from Andrews (2003) for $\alpha = 0.05$, $\pi_0 = 0.25$ (2) $SupLM_{0.95}$ is the 95-percentile of the SupLM statistics, (3) mean, min, max and sd are statistics retrieved from the 95% confidence intervals of the SupLM statistics, (4) K-mean re-groups the SupLM statistics obtained when combining all rounds in max 3 clusters, power, mean, min, max and sd are retrieved from the clusters, (5) N=3, (6) percentage change on W,A,B: (+20%), R: (+300%) and α and β: (+700%).

4. Empirical Results

We consider the daily returns of the MSCI Country Equity index (S) and the FTSE World Government Bond index[12] (B) of 22 advanced (AE) and 13 emerging (EME) economies. The list of Bloomberg tickers and the economic classification are reported in the Appendix, Table 8. We compute the average of the daily returns and construct 4 indices, i.e. $S.AE$, $S.EME$, $B.AE$ and $B.EME$. With data from 2006/01/04 - 2022/10/12, we account for 4,375 observations.

We perform the $TSSA$ to estimate the distinct breaking dates with $L = 1,000$, the trimming settled at 0.25 and $\wp = 0.95$. We compute the overlapped CI's among all the combinations of parameters, the corresponding estimated mean positions and standard deviations[13].

The first estimated date is the 2010/04/09, common to all the covariance parameters, with a standard deviation of +/-28 days. The second is the 2013/05/29 (+/-5) affecting the variance term A and the correlation structure (R, α and β). We detect another break only in the variance parameter A the 2015/11/03 (+/-11). Since this is the last estimated break in the variance structure, we account for this date to stack the estimated volatility from this point until the end of the sample. As follows we find a last break, the 2020/03/23 (+/-98 days), common to all the correlation parameters.

These dates can be related to the early stage of the European Sovereign Debt Crisis in 2011-2012, the Tapper Tantrum of 2013 originated in United States and the Covid-19 crisis[14].

---

[12]The FTSE World Government Bond selected tickers correspond to long-run bonds dominated in foreign currency.

[13]We make use of the CI's that result from the k-mean clustering when $\%power_k \geq 0.6$.

[14]Is it worth mentioning that since our sample finishes the 2022/02/02 and, given the required

In Table 6 we report the estimated parameters for the three distinct estimated dates enumerated above. We also present their p–value and the percentage change of the unconditional correlations with respect to the previous regime. The p–values are considerably small in almost all the cases, except for the variance constant term. Despite W not being significant, we keep it in the model to avoid the conditional variance to decrease over time[15].

By observing the estimated volatility parameters, we infer high level of persistence in all the sample period. The first volatility break is the 2010/04/09, common to all the parameters. We find that $B.AE$ and $S.EME$ become more sensitive to their own previous shocks ($\triangle A_{B.AE}$=+38% and $\triangle A_{S.EME}$=+71%). Conversely, the second regime gives rise to a negative shift for $B.EME$ ($\triangle A_{B.EME}$=-7%). The adjustment to past volatility (B), moves in opposite direction to A, preserving, this way, high level of persistence. The third regime implies a new structural change in the variance of the volatility (A). For the advanced economies, the parameters are significant and remain at high levels ($A_{S.AE} = 0.1360$ and $A_{B.AE} = 0.2021$). The last break found in A is the 2015/11/03. This last break is considered when estimating the model parameters during the fourth regime. Note that, during this last regime, $A_{S.AE}$ and $A_{B.EME}$ remains significant, though the shift with respect to the previous regime is more pronounced in

trimming settled at $\pi_0 = 0.25$, we are not able to detect structural breaks that may have occur after this date like the outbreak of the war in Ukraine or the hike of interest rates due to quantitative tightening in advanced economies.

[15]Note that the sum of GARCH coefficients (a_n and b_n) is less than one due to the stationary condition. Also, note that the estimated values are very close to zero. In this sense, $H0 : intercept = 0$ is testing a hypothesis that the parameter is on the boundary of the space. This might have implications on the null distribution of the test statistic, making the regular p-value associated with the t-statistic inappropriate. For that reason, we abstain from interpreting the estimated breaks found at W.

the emerging economies (-15% vs. +119% respectively).

The correlation structure appears to be time-varying during all the sample period with α and β highly significant. As noticed in Aielli (2013), for typical values of the dynamic parameters, i.e. $\alpha + \beta \leq 0.80$ and $\alpha \geq 0.16$, the DCC-GARCH estimates are well performed. The higher the impact of innovations, measured by α, the higher the variance of the correlation process. In this sense, α increases during the second regime, remains almost constant during the third one and decreases again during the last period.

We find distinct sings and shifts among the detected regimes in the cross-country and cross-market constant correlations. The sign of the correlations, as well as the sign of their percentage change, enable us to make conjectures about the way the AE and EME are interconnected.

Among all the period considered, we observe that constant correlations between the stock and government bond market have different signs within the advanced and emerging economies. For the former, the positive correlation between $S.AE$ and $B.AE$ may be explained by borrowing costs impacting on the companies' dividends (see Christiansen & Ranaldo, 2007). Conversely, for the emerging economies, changes in the local borrowing costs prompt capital flows, leading to pro-cyclical macroeconomic policies. As follows, mismatches in the aggregate demand trigger adjustments in the private companies' earnings (see Kaminsky et al., 2004).

The correlations between AE and EME also have different signs within the stock and the bond market among all the sample period. Within the stock market, the negative correlation can be explained by the counter-cyclical macroeconomic response to capital flows. In this sense, a rising stock market in the AE, may lead to risk averse portfolio rebalancing and, thus, a sell-of in the $S.EME$. The positive correlation within the bond market is related to global borrowing costs affecting the government debt burdens and, by doing so, the emerging countries' risk premium (see Garcia Herrero, 2011).

We observe significant shifts among the first and second regime. Since the European

Sovereign Debt Crisis took place in mid-2010, the rising default expectation among the euro area led to higher refinancing costs for private companies. In addition, liquidity squeeze in the credit market implied a decline in the investment and consumption (see Bauer, 2011). In this sense, we find that in the advanced economies the correlations between the stock and bond market increases ($\triangle R_{S.AE,B.AE}$= +66%). As noticed in Lane & Milesi-Ferretti (2017), capital flows to EME deepened after the European Sovereign Debt Crisis until 2013, giving rise to an increased foreign investor participation in their debt burden. As follows, the public and private sector in emerging countries became more sensitive to external borrowing costs (see López & Stracca, 2021). Likewise, we observe a shift in $B.AE$ and $B.EME$ ($\triangle R_{B.AE,B.EME} = +53\%$) and a decrease in $S.EME$ and $B.AE$ ($\triangle R_{S.EME,B.AE} = -30\%$) correlations. Volatility in the advanced economies can explain a moderate response of foreign investors positioned in EME to changes in the $S.AE$ returns. Therefore, we find a dimmer negative correlation within the stock markets ($R_{S.AE,S.EME}$ changes from -0.3297 to -0.2173) and a positive shift between $S.AE$ and $B.EME$ ($\triangle R_{S.AE,B.EME} = +20\%$).

The beginning of the third regime can be related to the FED announcement during the meeting in mid-2013. In that occasion, the FED showed the intention of taper the asset purchase program. As follows, long-term bonds and equity markets presented sell-off episodes close to the following meeting dates. In that respect, we observe a positive shift in correlations within the advanced economies markets ($R_{S.AE,B.AE}$ +42%). As noticed in Ahmed et al. (2017), the most adverse effects of U.S. monetary policy normalization were observed in the EME, who presented considerable sudden stops in portfolio flows reacting to increasing interest yields in advanced economies.

In the second part of the third regime, interest yields in advanced economies damped in response to the announcement of the ECB quantitative easing program in mid-2015. As follows, net capital flows to EME began to recuperate although they remained in negative territory (see IMF, 2016). Even though we observe similar dynamics as of the second regime (when high market integration took place), the negative net capital flows to EME seem to have a particular effect in the interconnection between the $B.EME$ and the stock market. When net capital inflows are negative, rising local interest yields is less effective to capture foreign capital and the negative impact in the aggregate demand predominates (see Kaminsky et al., 2004). In accordance, we find a dimmer negative correlation between the $S.EME$ and $B.EME$ ($R_{S.EME,B.EME}$=-0.0558). Analogously, the difficulty in damming outflows by increasing interest yields, for example in response to rising $S.AE$, may explain the less positive correlation between $S.AE$ and $B.EME$ ($\triangle R_{S.AE,B.EME}$=-32%).

The last regime coincides with the Covid-19 pandemic. We can distinguish three correlation shifts that presented a different sign with respect to the previous ones. Possibly explained by the emergency purchase programs oriented to mitigate financial instability, we find a decrease in the positive correlations between the stock and bond market in advanced economies ($\triangle R_{S.AE,B.AE}$= -13%). The second one is the noticeable negative correlation shift between advanced and emerging countries ($\triangle R_{S.AE,S.EME}$=1,034%), likely corresponding to a stronger flight-to-quality mechanism within the stock markets. As noticed in López & Stracca (2021), even though EME's cyclical position at the time of the Covid-19 shock left room for policy easing, the shock in the aggregate demand combined with sudden stops in capital flows, could not stop the equity market to fall. In that respect, the last notable shift is the increment in the correlations between $S.EME$ and $B.EME$ ($\triangle R_{S.EME,B.EME}$=+113%).

Table 6: Empirical Results - Estimated Parameters

	[1] [2006/01/04-2010/04/09]	[2] [2010/04/09-2013/05/29]	[3] [2013/05/29-2020/03/23]	[4] [2020/03/23-2022/10/12]
Variance Parameters				
$W_{S.AE}$	0.0000	0.0000	0.0000****	0.0000
$A_{S.AE}$	0.1292****	0.0790	0.1360****	0.1162****
$B_{S.AE}$	0.8497****	0.9093****	0.8162****	0.8494****
$W_{B.AE}$	0.0000	0.0000	0.0000	0.0000
$A_{B.AE}$	0.1445*	0.2000*	0.2021**	0.2648
$B_{B.AE}$	0.8455****	0.8126****	0.7771****	0.8006****
$W_{S.EME}$	0.0000	0.0000	0.0000	0.0000
$A_{S.EME}$	0.0368*	0.0628*	0.0368	0.0614
$B_{S.EME}$	0.9604****	0.9109****	0.9489****	0.9294****
$W_{B.EME}$	0.0000	0.0000	0.0000	0.0000
$A_{B.EME}$	0.0879****	0.0813*	0.0656*	0.1437***
$B_{B.EME}$	0.9023****	0.9075****	0.9313****	0.8445****
Correlation Parameters				
α	0.0182****	0.0287****	0.0274****	0.0018****
β	0.9658****	0.8689****	0.9326****	0.9171****
$R_{S.AE,B.AE}$	0.2466	0.4093 [66%]	0.5827 [42%]	0.5075 [-13%]
$R_{S.EME,B.EME}$	-0.2504	-0.2488 [-1%]	-0.0558 [-78%]	-0.1186 [113%]
$R_{S.AE,S.EME}$	-0.3297	-0.2173 [-34%]	-0.0131 [-94%]	-0.1489 [1,034%]
$R_{B.AE,B.EME}$	0.1338	0.2049 [53%]	0.3087 [51%]	0.3208 [4%]
$R_{S.AE,B.EME}$	0.4704	0.5652 [20%]	0.3818 [-32%]	0.4975 [30%]
$R_{S.EME,B.AE}$	0.3263	0.2274 [-30%]	0.2120 [-7%]	0.0554 [-74%]

Notes:(a) p-values: *$\leq$ 0.05, **$\leq$ 0.01, *** $\leq$ 0.001 and ****$\leq$ 0.0001 (b) the percentage changes with respect to the previous regimes are denoted in brackets [%].

5. Conclusion

This paper proposes a new *three-step segmentation algorithm* ($TSSA$) that tests for contagion with three distinct features. First, it is able to detect and date multiple breaks affecting each covariance term individually. Second it permits to capture common and distinct breaks affecting successively specific sets of parameters. Third, it prevents biases in the estimated correlations (by correcting for heteroscedasticity and possible structural changes in the variance structure) and enables to differentiate increased volatility from $shift - contagion$. This is because we perform the second stage of the DCC-GARCH estimation procedure by accounting for the structural breaks found in the variance terms. Third, by employing the $SupLM$ statistic, the $TSSA$ is computationally efficient. This is due to the fact that: (1) the LM employs the estimated parameters under the null, thus, the parameter estimation is performed only after the detected breaks and not for each sample partition, and (2) the $SupLM$ statistic makes use of the score functions of the restricted model.

Monte Carlo experiments show that the $TSSA$ has high testing power and it is able to locate the dates of contagion precisely. This is the case when one or more breaking dates affect a single set, or sequentially, all the model parameters. We notice that the standard $SupLM$ procedure proposed in Andrews (1993) can be seen as special case of the $TSSA$ when one breaking point is assumed to take place. In this sense, we prove that the $SupLM$ test performs properly under the DCC-GARCH framework with monotonic power. The results are consistent when the true breaking point is located in any of the extremes (always inside the boundary Π), though some power is diluted when the dimension of the portfolio increases. Finally, we note that, compared with the $SupLM$, the $TSSA$ still possess good power, even though the sample periods shrink after each detected break.

Our empirical study offers some new insights into the way advanced and emerging economies are interconnected within their goverment bond and equity market. The estimated breaking dates suggest common shifts in the correlation parameters after the early stage of the European Sovereign Debt Crisis, the Tapper Tantrum originated in United States in mid-2013 and the Covid-19 crisis. We observe a single isolated structural break for one variance parameter (A) in November 2015. The peculiar sign in the stock and bond market correlation within the EME supports the evidence that net capital inflows are strongly linked with monetary policy decisions and macro fundamentals. In this line, we find signs of contagion between $B.AE - B.EME$, possibly driven by fluctuations in the global borrowing costs. We detect negative correlations between $S.EME - B.EME$ and $S.AE - S.EME$ addressing *flight-to-quality* dynamics. However, these correlations increase until the point that they become close to zero during the third regime, supporting the hypothesis that the macroeconomic response to capital flows is counter-cyclical in EME. Future research can be conducted to detect possible changes in the interconnection of these market after the war in Ukraine and the subsequent quantitative tightening conducted by several AE.

Further applications of the $TSSA$ could be done in other time series models such as Vector Autoregressive models with GARCH errors, where the detection of structural changes in the mean structure can preside the step targeted to the covariance terms. Furthermore, the $TSSA$ could be applied to the cDCC model introduced in Aielli (2013), more tractable under typical values of the dynamic parameters, i.e. $\alpha + \beta \leq 0.80$ and $\alpha \geq 0.16$. Finally, forecasting techniques on time series accounting for the presence of in-sample structural breaks could also incorporate this procedure.

6. Appendix

Table 7: Parameter values for the simulated series under H0 and H1

	W	A	B	R	α	β
Under H0						
	0.300	0.300	0.300	0.100	0.050	0.050
Under H1						
Monte Carlo Experiments (i)-(iv)						
SMALL	0.450	0.450	0.450	0.300	0.300	0.300
	[50%]	[50%]	[50%]	[200%]	[500%]	[500%]
MEDIUM	0.600	0.600	0.600	0.350	0.350	0.350
	[100%]	[100%]	[100%]	[250%]	[600%]	[600%]
LARGE	0.675	0.675	0.675	0.400	0.400	0.400
	[125%]	[125%]	[125%]	[300%]	[700%]	[700%]
Monte Carlo Experiment (v)						
	0.360	0.360	0.360	0.400	0.400	0.40
	[20%]	[20%]	[20%]	[300%]	[700%]	[700%]

Notes: [.%] denotes the percentage change with respect to the parameter values under the null hypothesis.

Table 8: List of selected Bloomberg Tickers per market and economy

Country	Stock	Bond
AE		
Australia	MXAU Index	SBADL Index
Austria	MXAT Index	SBASC Index
Belgium	MXBE Index	SBBFL Index
Canada	EWC US Equity	SBCDUKC Index
Denmark	MXDK Index	SBDKEC Index
Finland	MXFI Index	SBFMEU Index
France	MXFR Index	SBFFL Index
Germany	MXDE Index	SBDML Index
Ireland	MXIE Index	SBIRL Index
Israel	MXIL Index	SBIS70L Index
Italy	MXIT Index	SBITL Index
Japan	MXJP Index	SBJYL Index
Netherlands	MXNL Index	SBDGL Index
New Zealand	MXNZ Index	SBNZL Index
Norway	MXNO Index	SBNKL Index
Portugal	MXPT Index	SBPEL Index
Singapore	MXSG Index	SBSGL Index
Spain	MXES Index	SBSPL Index
Sweden	MXSE Index	SBSKL Index
Switzerland	MXCH Index	SBSZL Index
United Kingdom	MXGB Index	SBUKL Index
United States	MXUS Index	SBUSL Index
EME		
China	MXCN Index	SBCNL Index
Greece	MXGR Index	SBGRL Index
Hungary	MXHU Index	SBHUL Index
India	MXIN Index	SBINY Index
Indonesia	MXID Index	SBIDL Index
Korea	MXKR Index	SBKRL Index
Malaysia	MXMY Index	SBMYL Index
Mexico	MXMX Index	SBMXL Index
Philippines	MXPH Index	SBPHL Index
Poland	MXPL Index	SBPLL Index
Russia	MXRU Index	SBRU13L Index
South Africa	MXZA Index	SBZAY Index
Turkey	MXTR Index	SBTRL Index

Note: The countries are classified into advanced (AE) and emerging (EME) economies based on the MSCI Annual Market Classification of June 2021 referring respectively to the category of developed and emerging markets.

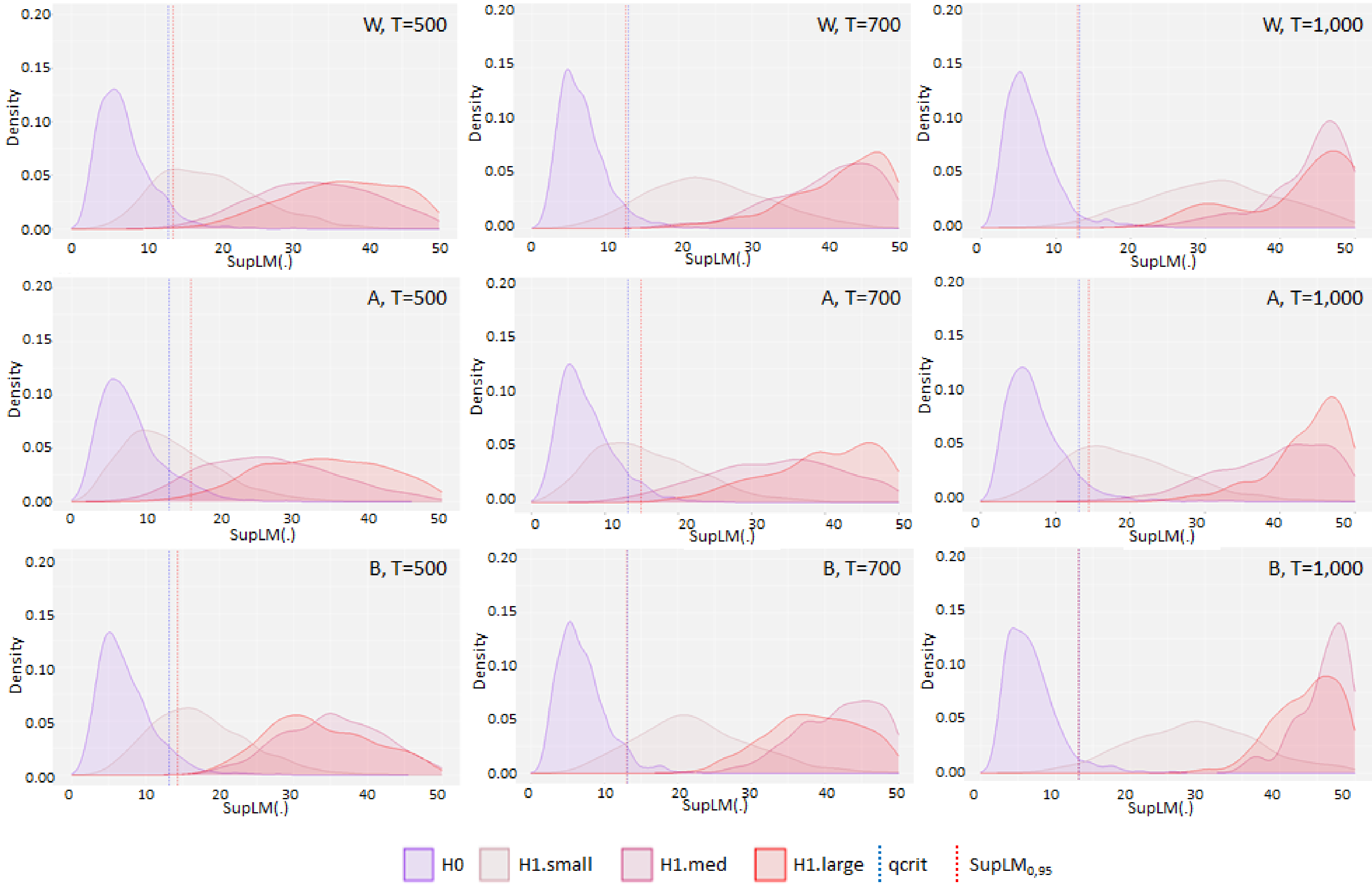

Figure 1: (i) experiment: small, medium and large changes affecting each parameter one by one (1/2)

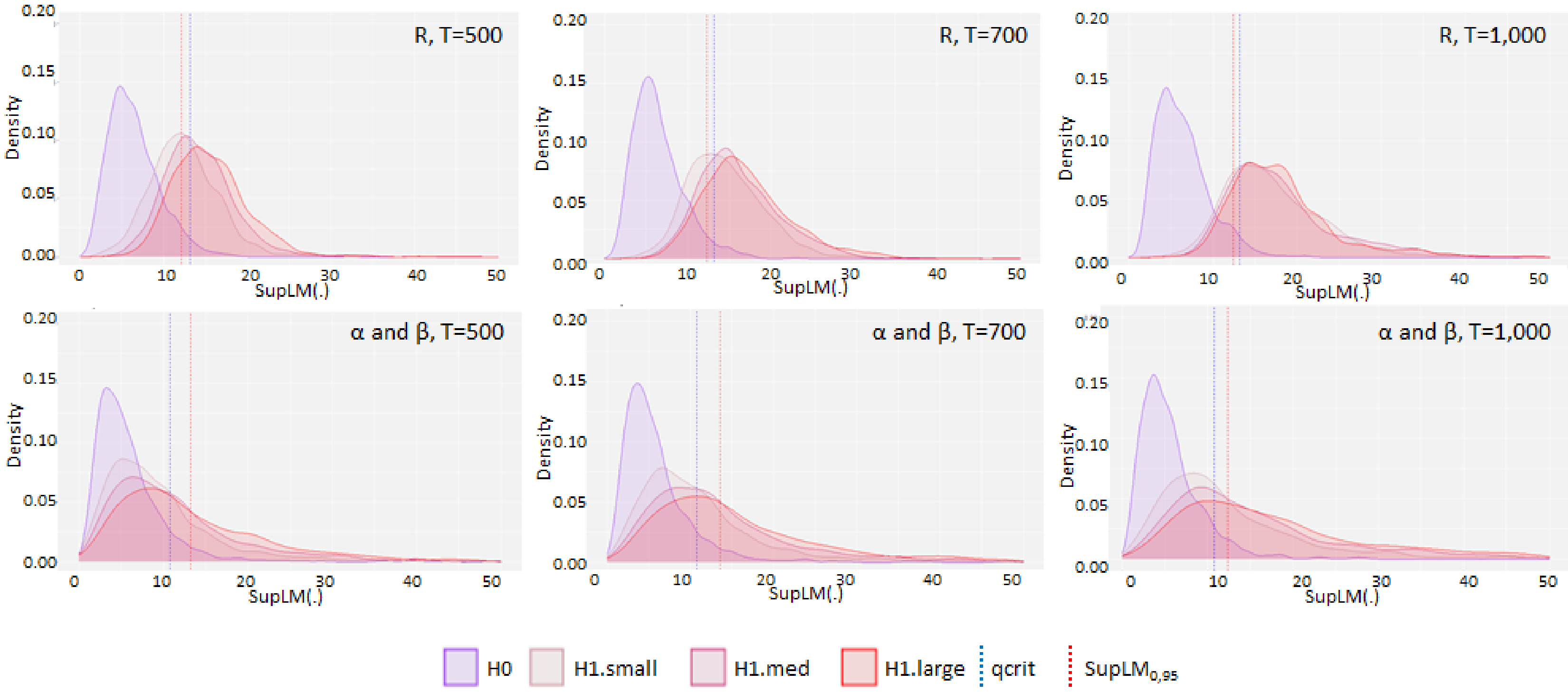

Figure 2: (i) experiment: small, medium and large changes affecting each parameter one by one (2/2)

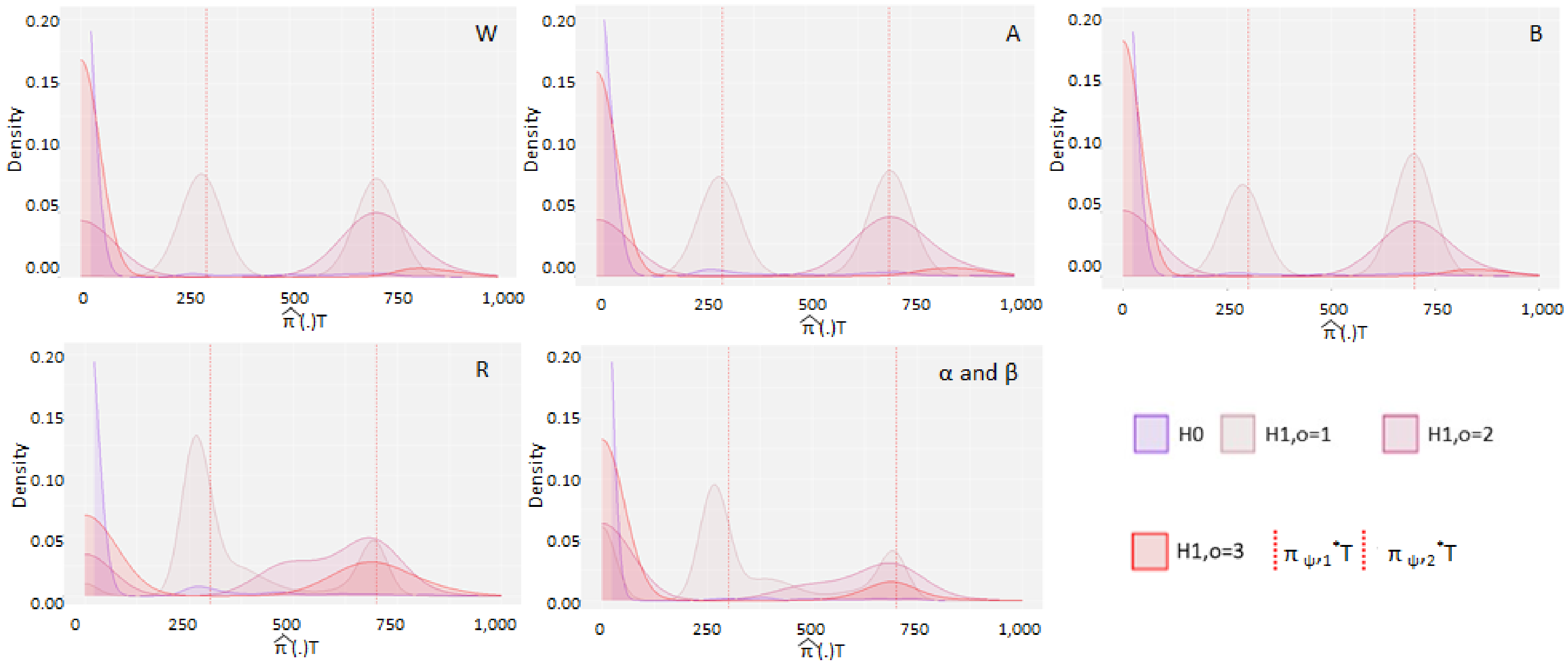

Figure 3: (iv) experiment: two successive breaks affecting each parameter one by one

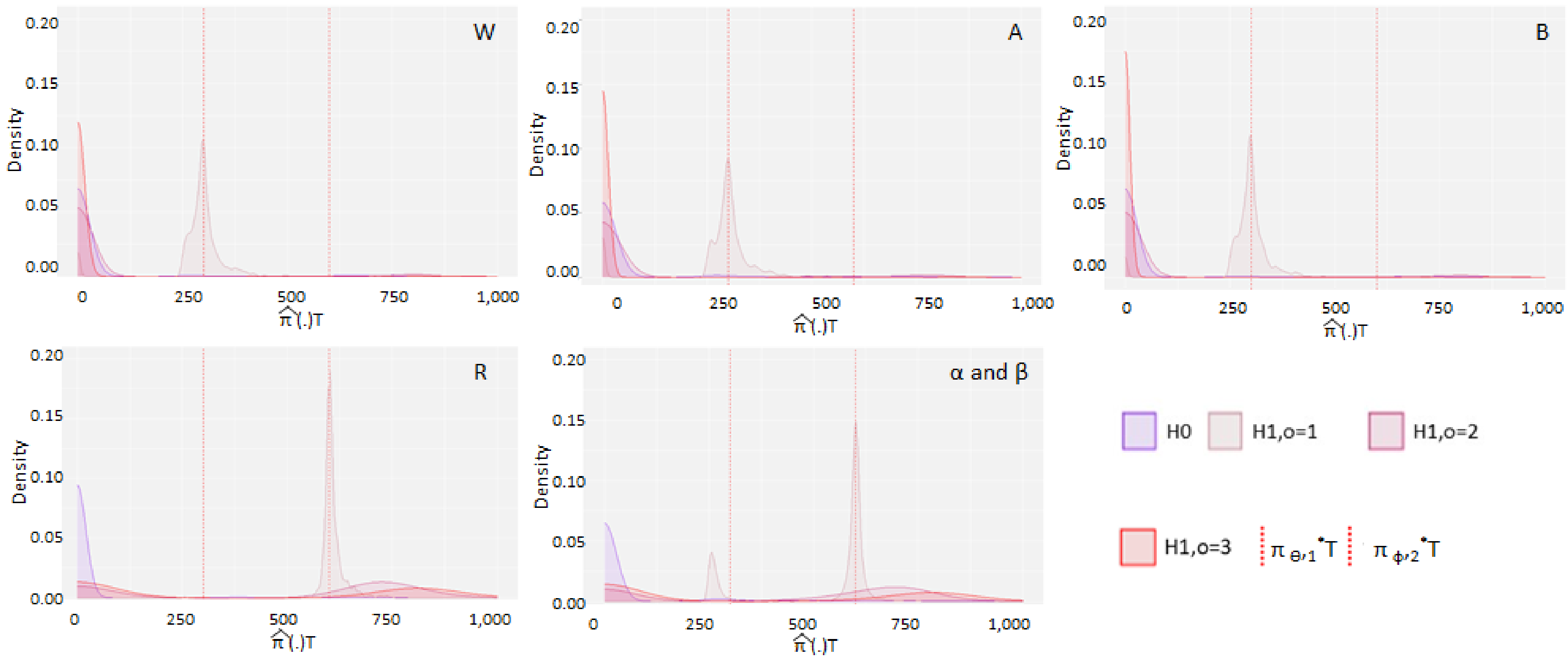

Figure 4: (v) experiment: two successive breaks affecting $\theta = [W, A, B]$ ($\pi_1 = 0.3$) and $\phi = [R, \alpha, \beta]$ ($\pi_1 = 0.7$)

References

Adams, Z., Füss, R., & Glück, T. (2017). Are correlations constant? empirical and theoretical results on popular correlation models in finance. *Journal of Banking & Finance*, 84, 9–24. https://doi.org//10.1016/j.jbankfin.2017.07.003

Ahmed, S., Coulibaly, B., & Zlate, A. (2017). International financial spillovers to emerging market economies: How important are economic fundamentals? *Journal of International Money and Finance*, 76, 133–152.

Aielli, G. P. (2013). Dynamic conditional correlation: on properties and estimation. *Journal of Business & Economic Statistics*, 31(3), 282–299. https://doi.org/10.1080/07350015.2013.771027

Andrews, D. W. (1993). Tests for parameter instability and structural change with unknown change point. *Econometrica: Journal of the Econometric Society*, 821–856. https://doi.org//10.2307/2951764

Andrews, D. W. (2003). Tests for parameter instability and structural change with unknown change point: A corrigendum. *Econometrica*, 395–397. https://www.jstor.org/stable/3082056

Andrews, D. W. & Ploberger, W. (1994). Optimal tests when a nuisance parameter is present only under the alternative. *Econometrica: Journal of the Econometric Society*, 1383–1414. https://doi.org//10.2307/2951753

Bai, J. (1993). Estimation of structural change based on wald-type statistics.

Bai, J. & Perron, P. (1998). Estimating and testing linear models with multiple structural changes. *Econometrica*, 47–78. https://doi.org//10.2307/2998540

Bauer, L. R. (2011). Debt and currency crises. In Kolb (2011).

Baur, D. G. & Lucey, B. M. (2009). Flights and contagion – an empirical analysis of stock–bond correlations. *Journal of Financial stability*, 5(4), 339–352. https://doi.org//10.1016/j.jfs.2008.08.001

Beirne, J. & Gieck, J. (2014). Interdependence and contagion in global asset markets. *Review of International Economics*, 22(4), 639–659. https://doi.org/10.1111/roie.12116

Blatt, D., Candelon, B., & Manner, H. (2015). Detecting contagion in a multivariate time series system: An application to sovereign bond markets in europe. *Journal of Banking & Finance*, 59, 1–13. https://doi.org//10.1016/j.jbankfin.2015.06.003

Cho, J.-W., Choi, J. H., Kim, T., & Kim, W. (2016). Flight-to-quality and correlation between currency and stock returns. *Journal of Banking & Finance*, 62, 191–212. https://doi.org/10.1016/j.jbankfin.2014.09.003

Choe, K.-i., Choi, P., Nam, K., & Vahid, F. (2012). Testing financial contagion on heteroskedastic asset returns in time-varying conditional correlation. *Pacific-Basin Finance Journal*, 20(2), 271–291. https://doi.org/10.1016/j.pacfin.2011.09.003

Christiansen, C. & Ranaldo, A. (2007). Realized bond - stock correlation: Macroeconomic announcement effects. *Journal of Futures Markets: Futures, Options, and Other Derivative Products*, 27(5), 439–469. https://doi.org/10.2139/ssrn.746364

Engle, R. (2002). Dynamic conditional correlation: A simple class of multivariate generalized autoregressive conditional heteroskedasticity models. *Journal of Business & Economic Statistics*, 20(3), 339–350. https://doi.org/10.1198/073500102288618487

Engle, R. F. (2009). High dimension dynamic correlations. *The Methodology and Practice of Econometrics: Festscrift for David Hendryâ, Oxford University Press, USA*, 122–148. https://doi.org/10.1093/acprof:oso/9780199237197.003.0005

Estrada, F., Tol, R. S., & Gay-García, C. (2015). The persistence of shocks in gdp and the estimation of the potential economic costs of climate change. *Environmental Modelling & Software*, 69, 155–165. https://doi.org/10.1016/j.envsoft.2015.03.010

Forbes & Rigobon, R. (2002). No contagion, only interdependence: Measuring stock market comovements. *Journal of Finance*, 57(5), 2223–2261. https://doi.org//10.1111/0022-1082.00494

Galeano, P. & Tsay, R. S. (2010). Shifts in individual parameters of a garch model. *Journal of Financial Econometrics*, 8(1), 122–153. https://doi.org/10.1093/JJFINEC/NBP007

Garcia Herrero, A. (2011). Emerging countries' sovereign risk: Balance sheet effects, global risk aversion, and contagion. In Kolb (2011).

Hafner, C. M. & Herwartz, H. (2008). Analytical quasi maximum likelihood inference in multivariate volatility models. *Metrika*, 67(2), 219–239. https://doi.org//10.1007/s00184-007-0130-y

Hartigan, J. A. & Wong, M. A. (1979). Algorithm as 136: A k-means clustering algorithm. *Journal of the royal statistical society. series c (applied statistics)*, 28(1), 100–108. https://doi.org/10.2307/2346830

Hillebrand, E. (2005). Neglecting parameter changes in garch models. *Journal of Econometrics*, 129(1-2), 121–138. https://doi.org//10.1016/j.jeconom.2004.09.005

IMF (October 2016). *World economic outlook: Subdued demand - symptoms and remedies*.

Kaminsky, G. L., Reinhart, C. M., & Végh, C. A. (2004). When it rains, it pours: procyclical capital flows and macroeconomic policies. *NBER macroeconomics annual*, 19, 11–53. https://www.jstor.org/stable/3585327

Kolb, R. (2011). *Financial contagion: the viral threat to the wealth of nations*, volume 604. John Wiley & Sons.

Lane, M. P. R. & Milesi-Ferretti, M. G. M. (2017). *International financial integration in the aftermath of the global financial crisis*. International Monetary Fund. https://doi.org/10.5089/9781484300336.001

López, G. G. & Stracca, L. (2021). Changing patterns of capital flows. *CGFS BIS Working Paper*, (66).

Oka, T. & Perron, P. (2018). Testing for common breaks in a multiple equations system. *Journal of Econometrics*, 204(1), 66–85. https://doi.org/10.1016

Perron, P. et al. (2006). Dealing with structural breaks. *Palgrave handbook of econometrics*, 1(2), 278–352.

Rigobon, R. (2019). Contagion, spillover, and interdependence. *Economía*, 19(2), 69–100. https://www.jstor.org/stable/26628926

Sobrun, J. & Turner, P. (2015). Bond markets and monetary policy dilemmas for the emerging markets. *BIS Working Paper*, (NO 508). https://ssrn.com/abstract=2641091

Vogelsang, T. J. (1999). Sources of nonmonotonic power when testing for a shift in mean of a dynamic time series. *Journal of Econometrics*, 88(2), 283–299. https://doi.org/10.1016/S0304-4076(98)00034-7